



The effects of chemical environment on the nucleation, growth, and stability of ettringite $[\text{Ca}_3\text{Al}(\text{OH})_6]_2(\text{SO}_4)_3 \cdot 26\text{H}_2\text{O}$

A.M. Cody^{a,*}, H. Lee^b, R.D. Cody^a, P.G. Spry^a

^aDepartment of Geological and Atmospheric Sciences, 253 Science I, Iowa State University, Ames, IA 50011-3210, USA

^bDepartment of Geology, College of Natural Sciences, Pusan National University, Pusan 609-735, South Korea

Received 21 April 2003; accepted 27 October 2003

Abstract

Ettringite is responsible for both the initial set of Portland cement and for premature concrete deterioration. A new method of ettringite crystal growth by combining calcium hydroxide and aluminum sulfate solutions was devised to reliably produce crystals that could be seen with a light microscope ($45 \times -320 \times$). The nucleation, growth, morphology, and stability of ettringite in the presence of over 300 chemicals and admixtures, many of which are present in the concrete environment, was then investigated. The plasticizers sorbitol, citrate, and tartrate were found to inhibit ettringite nucleation and growth, as did certain lignosulfonate air-entraining admixtures. The Type B set retarder borax inhibited ettringite formation at <44 ppm. The consequences and implications of this are discussed.

© 2004 Elsevier Ltd. All rights reserved.

Keywords: Ettringite; Chemical environment; Crystal size; Delayed ettringite formation (DEF); Stability

1. Introduction

In most Portland cements hydrated at $15-25^\circ\text{C}$ with a water/cement (w/c) ratio of 0.45–0.65, X-ray peaks of ettringite are detectable within a few hours and increase in intensity to a maximum in approximately 1 day [1]. Primary ettringite contributes to the early strength of concrete [2]. Because ettringite has a high water content of 46% by weight [3], its formation affects the consistency and workability of cement. Cements that are high in ettringite are used to produce products that dry rapidly and harden quickly [3].

In contrast, secondary or delayed ettringite, formed after concrete has hardened, is considered by many to be deleterious [4–7]. Delayed ettringite is believed to produce expansive forces attributed to one or more factors such as crystal growth forces, varied hydration, and/or adsorbed crystal surface water. Expansive forces may also be produced by ettringite filling of air-entrainment voids so that they no longer handle the expansive forces of ice crystals resulting from pore water freezing [6,8,9]. Expansive forces lead to cracking, strength loss, and disintegration of concrete [5,10,11]. The presence and properties of primary and

secondary ettringite are both determined by the chemical environment in the concrete.

Road deicers, fly ash, lignosulfonate and hydroxycarboxylic acid water reducers, plasticizers, superplasticizers, air-entrainment chemicals, environmental contaminants, and numerous other chemicals are present in the highway concrete environment. It is important to know the effects of these chemicals on the formation and stability of ettringite.

Several previous studies of ettringite formation [4,12,13] involve the reaction of solid components such as tricalcium aluminate (C_3A), tetracalcium aluminum sulfate ($\text{C}_4\text{A}_4\text{S}$), calcium sulfate (CS), and calcium hydroxide (CH) with water in a changing mixture containing many phases. To isolate and study only those reactions pertaining to the nucleation and growth of ettringite and the effects of environmental chemicals on those processes, it was necessary to grow the crystals from solution. Several previously published solution growth methods were initially tested.

The saccharate method of Carlson and Berman [14] produced crystals that were too small to see without high-magnification views with a scanning electron microscope (SEM). Crystals formed instantly because of the high concentration of reactants, showing that the method was not suitable for studying changes in nucleation rates. Over time, the final solution developed a brown color and exhibited green fluorescence in short wave UV light,

* Corresponding author.

E-mail address: amcody@iastate.edu (A.M. Cody).

indicating that sugar polymerization was occurring and could possibly interfere with the experiments.

The method of Mylius [15], as described in Taylor [1], also produced small crystals needing a SEM magnification of $2000\times$ to be seen. The induction time, or the time between the combining of solutions and the first appearance of crystals was ≈ 45 s, more suitable for nucleation rate studies. This method, however, was not found to be reliable in producing ettringite. Calcium aluminate monosulfate (AFm/monosulfate) sometimes formed. Therefore, it was necessary to devise a new method of crystal growth for the present study.

2. Experimental

All solutions were made with double-distilled, deionized water, and filtered with Whatman #43 paper to remove any crystalline material. A saturated solution of calcium hydroxide (≈ 1.85 g/l) was made by adding excess CaO to distilled water, stirring the covered solution for 2 h with a magnetic stir bar and then filtering the liquid. Calcium hydroxide solution was stored in a thick polypropylene container with a bottom tap. Air that entered the container was bubbled through a carbon dioxide lock containing limewater [$\text{Ca}(\text{OH})_2$] to remove CO_2 . An aluminum sulfate solution was produced by adding 2.417 g of $\text{Al}_2(\text{SO}_4)_3 \cdot 18\text{H}_2\text{O}$ to 1 L of distilled water followed by filtering. The relative quantities of ions in this crystal growth method are not stoichiometric, but blank solutions reliably produced elongate six-sided ettringite crystals that are visible with a light microscope ($45\times$ – $320\times$). Reactions in blank solutions have an induction time of approximately 1 min and no intermediate gel phase was ever observed. In most cases, 25 ml of aluminum sulfate solution were placed in a hard plastic container with a chemical additive and swirled to dissolve the additive. Then 20 ml of saturated $\text{Ca}(\text{OH})_2$ solution were added to nearly fill the container and minimize CO_2 contamination. The container was then capped and its contents swirled. In some cases where a precipitate could form in the $\text{Al}_2(\text{SO}_4)_3$ solution, the additive was mixed with the $\text{Ca}(\text{OH})_2$ solution and the sulfate solution was then added.

Ettringite is generally stable in the pH range 10.5 to 13.0 [16]. For additives that produced a pH below 10.5, pH was adjusted with 5 M NaOH. The containers were left for 24 h, then the contents of containers with visible precipitate were filtered through Whatman #40 filter paper, rinsed with a small quantity of distilled water, and the crystals were examined with a petrographic microscope. Crystal morphology or outward appearance (needles: length, solitary/radiating, pointed/not; plates: size, single/clustered, 3/6 sides) and the relative amount of each phase were noted. The optic orientation and sign of needlelike crystals were determined. Crystals with

unusual morphology were tested with 10% HCl to determine if they were calcium carbonate, which was seen to form short six-sided optically negative prisms that resemble short ettringite crystals. The mineral composition of each morphology was determined by X-ray diffraction analysis with nickel-filtered $\text{CuK}\alpha$ radiation at 35 kV and 20 mA. Patterns were collected between 5.0° and 50.0° 2θ using an angle step of 0.05° and a dwell time of 0.5 s. Crystals were not crushed before X-ray to avoid carbonation and loss of water from highly hydrated phases. Low vacuum SEM and energy-dispersive X-ray analysis (EDAX) were used when necessary to distinguish the identity of forms in multiphase precipitates. The relative quantity of air-dried crystals [large (L), medium (M), small (S), trace (Tr)] was also recorded.

Between experiments the plastic containers used were cleaned with full-strength hydrochloric acid, rinsed several times with distilled water, and air-dried. Over 300 additives were tested for their effects on the nucleation and growth of ettringite.

3. Discussion and results

The effects of different additives on ettringite are not straightforward because considerable substitution in the basic ettringite formula $[\text{Ca}_3\text{Al}(\text{OH})_6]_2 \cdot 24\text{H}_2\text{O} \cdot (\text{SO}_4)_3 \cdot 2\text{H}_2\text{O}$ can occur (see Fig. 1 for crystal structure). Calcium can be replaced by Pb and Sr [17], Al by Cr, Si, Ti, Co, Mn, Fe, Ga, and Ge [14,17], and sulfate may be partly or completely replaced by CO_3^{2-} , CrO_4^{2-} , IO_3^- , and $\text{BO}_3^{2-}/\text{B}(\text{OH})_4$ [14,17,18]. The effects that these replacements have on the morphology and the stability of the aluminoferrite trisulfate (Aft), ettringite, phase deserve further attention.

Several general results can be expected from crystal growth experiments with additives:

1. No effect will be seen because the additive does not affect the nucleation or growth of the crystals.
2. Crystal nucleation may be affected.
 - a. Fewer crystals may form because nucleation is prevented.
 - b. Nucleation of ettringite ($K_{\text{sp}} = 2.80\text{e}^{-45}$ [16]) may be completely inhibited and another less stable mineral such as calcium aluminate monosulfate/AFm ($K_{\text{sp}} = 3.71\text{e}^{-30}$ [16]) may form instead.
 - c. Nucleation of all crystals may be inhibited and a gel/colloid may or may not form.
 - d. The additive may enhance nucleation causing a large number of extremely small crystals to form. When a large quantity of crystals nucleates, each individual crystal has less nutrient to grow to large size.
3. Crystal growth may be affected.
 - a. The additive may preferentially adhere to certain faces of the crystals and prevent or slow the addition of new layers of growth on those faces. When no

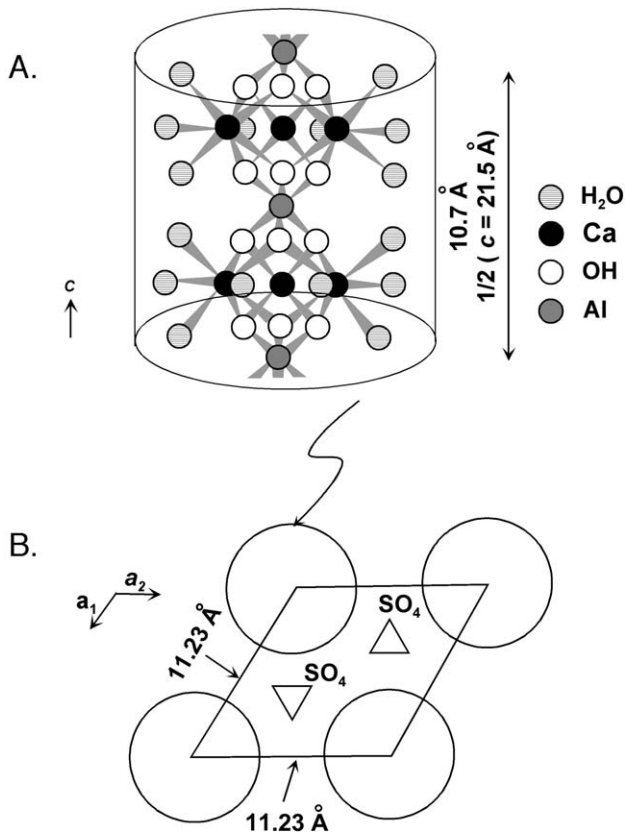


Fig. 1. Crystal structure of ettringite. (A) Structure of ettringite column, one-half unit cell. Structure is parallel to the c crystallographic axis (c spacing is 21.5 Å). Modified from Day [29]. (B) View of a - b plane. Circles represent ettringite columns; regions between columns are channels containing water and sulfate molecules. a_1 and a_2 unit cell spacings = 11.23 Å. Modified from Day [29] after Taylor [17].

additives are present, ettringite crystals exhibit six large elongate $\{10\bar{1}0\}$ rectangular prism faces and two flat, six-sided $\{0001\}$ end faces (Fig. 2A). (1) If an additive adsorbs only on the end faces, the elongate $\{10\bar{1}0\}$ side faces will continue to have new layers of growth deposited on them, and the resulting crystals will appear shorter and thicker. (2) If an additive adsorbs only on the rectangular prism faces, new growth layers will form more rapidly on the six-sided end faces, resulting in thin, elongate crystals.

- b. The additive may adsorb onto the edges between faces. (1) If adsorption occurs on the edges where the short sides of the rectangular $\{10\bar{1}0\}$ faces meet the six-sided $\{0001\}$ faces, pointed or rounded crystal tips may result (Fig. 2B). (2) Adsorption on the long edges between rectangular $\{10\bar{1}0\}$ faces produces the formation of new/rough faces between the rectangular faces (Fig. 2C).

The results of the experiments are shown in Table 1. Chemicals with similar functional groups (i.e., nitrates or carboxylates) are grouped to reveal general trends. The following groups were tested.

3.1. Ionic species

Different cations and anions were examined because their presence in concrete might be expected. Silica and magnesium are always present. Lithium salts and hydroxides of Ca and K are added as accelerators of set time; magnesium chloride and barium nitrate are also used to control set time. Sodium chloride and nitrate, potassium chloride and sulfate, calcium sulfate, as well as barium chloride are used to retard concrete set time [3]. Sodium nitrate is also added for its water-reducing effect.

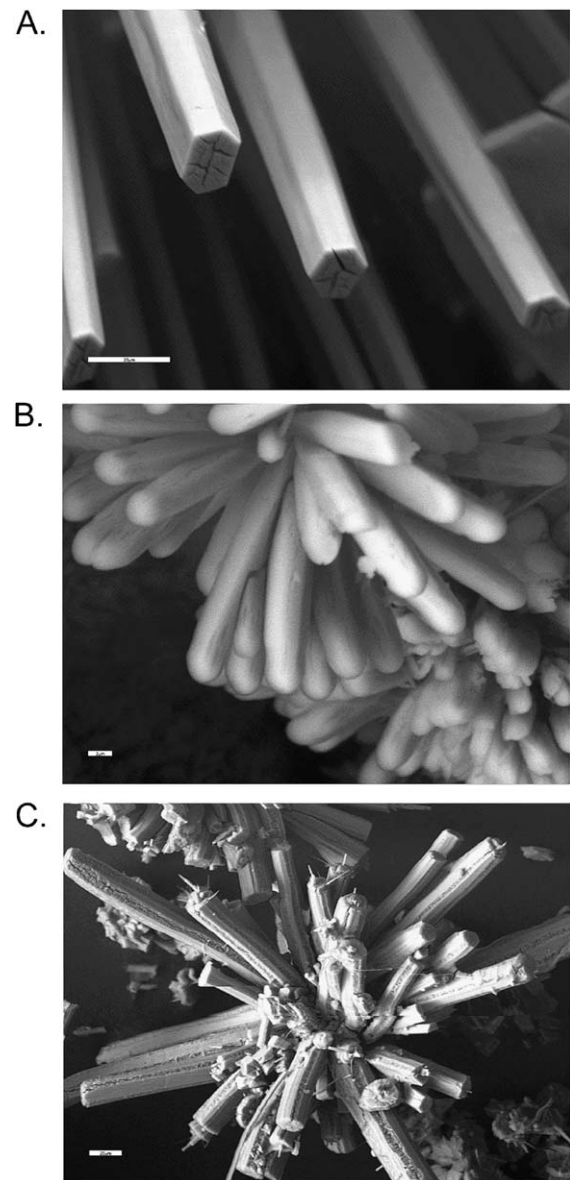


Fig. 2. Examples of synthetic ettringite. (A) Six-sided needle-like morphology of ettringite grown in solution without additives, showing elongate $\{10\bar{1}0\}$ and hexagonal $\{0001\}$. Bar = 20 μm . (B) Short, “pointed,” ettringite crystals formed with arabinic acid (Experiment 81). Bar = 2 μm . (C) Elongate, thin ettringite crystals grown with Alizarin Red S (Experiment 153) exhibit growth defects on their long edges. Bar = 20 μm .

Table 1
Summary of crystallization experimental results

Experiment No.	Chemical	Quantity of precipitate	Features
<i>Ionic species</i>			
A. Chlorides			
249	NH ₄	L	Long, thin fiberlike needles
195	Ba	M	Spheres—very long, med. thick needles
159	Co	L	Spheres—very thin needles and a few AFm spheres (plates)
171, 253	Cr		Clusters of a few long, very thin needles
198	Cu ⁺³	L	Probably pointed, spheres—large, with long (0.3 mm) needles
162	Li	L	Spheres—very long med. thin needles
17, 163	Mg	ML	Small spheres—thin, short (0.03 mm) needles and split calcite
18, 19, 247	Na	L	Experiment 18 (small amt. NaCl) spheres—small thin needles; Experiment 19 (large amt. NaCl) spheres—med. size long (0.25 mm) thin needles.
161	Pb	L	Probably pointed, spheres—very long, very thin needles
256	K	L	Med., long thin needles
165	Rb	L	Pointed, spheres—needles
217, 264	Sn	L	Med. long, med. thin needles
216, 291	Zn	M	Gel and colloidal precipitate

Table 1 (continued)

Experiment No.	Chemical	Quantity of precipitate	Features
209, 267	ZrO	L	Very long (0.2 mm) thin needles, probably pointed
B. Nonchlorides			
214	AgNO ₃	S	Pointed, dense spheres—med. long thin needles
197	CeNHNO ₃	L	Small, spheres—tiny, long needles
201	NiNO ₃	ML	Med. long, very thin needles
191, 266	TiKF ₂	L	Med. long, thin needles that hold much surface water
213	Silica gel	M	Spheres—med. long, thin needles
192	UAc	L	Dense spheres—med. long, thin needles
263	NaNO ₃	L	Med. long thin needles
	Na nitrite	L	Long thin needles
<i>Carboxylic acids/carboxylates and borates</i>			
4, 177, 215	Acetate, Na	M	Spheres—long large needles
160	Acetate, Pb	L	Very long, very thin needles
192	Acetate, U	L	Dense spheres—med. long thin needles; gel
28	EDTA	M	Med. long. med. thick needles
147	Acetate, Phenyl	M	Med. long, thin and med. long thick needles
5	Aconitic	S	Large, thick needles
178	Alginic, Na	L	Med. long, med. thick needles; some large calcite

Table 1 (continued)

Experiment No.	Chemical	Quantity of precipitate	Features
95, 276	L-Ascorbic	M	Ca oxalate dihydrate, short and med. long, med. thick crystals
158, 250	Boric acid	ML	Small (0.63 mm dia.) spheres—AFm plates
2, 259, 294, 295, 296	Borate, Na	L	Spheres, AFm and short (0.009 mm) thin needles
141	Cholic	L	Pointed, med. long, med. thick
7	Citrate, Na	S	Small, short needles
199	Citrate, Fe ⁺³	L	Spheres—long, thin needles, insoluble (?)
85	Isocitric	M	Short needles; some AFm
245	Citrate, NH ₄ dibasic	Tr	Short needles; calcite spherulites
83	Coumaric	L	Clumps—very long thin needles
142	Docosanoic	L	Med. long, med. thick needles and small thin needles
167	1,12-Docecanedicarboxylic	L	Spheres—med. long, thin needles
108, 279	Galacturonic	S	Spheres—short thick prisms
64, 261	Glutamic	M	Long, broad needles
31, 246	Glutamic, Na	M	Giant long, broad needles
182, 262	Glycolic, Na	M	Spheres—short, very thin needles
112	Thioglycolic, Na	M	0.04-mm needles
211	Maleic anhydride	M	Large spheres—med. long, med. thick needles
224, 254	Malic	L	Med. long, med. thin needles
145	Malonic, Na	M	Spheres—long (0.2 mm) med. wide needles

Table 1 (continued)

Experiment No.	Chemical	Quantity of precipitate	Features
36, 212, 243, 245, 288, 289, 292	Mucic/galactaric	Tr	Gel; tr. calcite
125, 202	Nicotinic	M	Spheres—med. long, med. thin needles
203	O-Nitrobenzoic	ML	Spheres—long, med. long, med. thick needles
89	Nucleic	L	Large, very long needles
146	Orotic	M	Spheres—long, med. thick and thin needles
9	Oxalic, K	M	Needles; Ca oxalate dihydrate
175	M-phosphoric	L	Spheres—small thin needles
166, 218	Salicylic	M	Long, broad needles; tr. AFm and calcite
72	Shikimic	M	Med. long, wide needles
149	Sorbic	L	Med. long, thin needles
150	Suberic	M	Med. long, med. thick needles and med. long, thin needles
183	Succinic	L	Med. long, med. thick needles
186	Succinate, Na	ML	Very long (0.37 mm), med. thick needles
26	Tannic	L	Clumps—large needles; tr. gypsum
274	Tartaric, NH ₄	S	Clusters—short thick crystals
3, 281	Tartaric, K	M	Clusters—short and med. long thick crystals
184, 286	Tartaric, Na	M	Clusters—short and med. long med. thick crystals

(continued on next page)

Table 1 (continued)

Experiment No.	Chemical	Quantity of precipitate	Features
34	Uric	M	Clusters—med. long, small elongate needles
<i>Amino acids + NH₂ compounds</i>			
91, 92	D-Alanine	Tr	Spheres—long and med. needles
93	L-Arginine	ML	Long, very thin needles
82, 115	L-Asparagine	M	Clusters—med. long needles with pointed tips; gel
94, 276	L-Aspartic acid	L	Clusters—med. long, med. thick needles
98	L-Cystine	M	Clusters—short, thin needles
103	D-Glutamic acid	M	Few short, thin needles; large calcite
104, 261, 280	L-Glutamic acid	L	Spheres—long ultra-thin needles
31, 260	Glutamate, Na	L	Spheres—long ultra-thin needles
105, 144	Glycine	LM	Clusters—med. long, thick and thin needles
65	DL-Isoleucine	L	Clusters—long broad needles
66	D-Leucine	L	Clusters—med. wide needles
67	DL-lysine HCl	L	Med. long very thin needles
68	DL-Methionine	ML	Med. long thin needles
80	Ornithine HCl	Tr	Clusters—small thin pointed needles
69	DL-Phenylalanine	L	Med. long (0.12 mm) thin needles
70	Protamine sulfate	L	Clumps—long, very thin needles
198, 273	L-Pyroglutamic acid	L	Long, thin needles
74	D-Threonine	L	Large clumps—very thin needles

Table 1 (continued)

Experiment No.	Chemical	Quantity of precipitate	Features
137, 265	Thiopropine	L	Long med. thick needles (optically +)
87	Tricine	L	Spheres—long thick needles
75	DL-Tryptophan	L	Spheres—very thin long needles
139, 270	Adenosine	L	Long thin needles
101	D-Dianisidine	S	Clusters—med. long thin needles
151,188	Sulfanilic	M	Small thin needles
257	Sulfathiazole	VL	Ultra-long very thin needles
187, 287	Sulfamic acid	L	Long (0.3 mm) thin needles
207	DL-Barbital, Na	L	Spheres—long thin needles
33	Urea	S	Spheres—thin needles
<i>Purines and related substances</i>			
114	Adenine	ML	Many clusters—long thin needles
118	Guanine	L	Long thin needles
121	Hypoxanthine	M	Long thin needles
78	Xanthine	M	Very long thin and thick needles
6, 251	Caffeine	L	Med. long, med. thin needles
84	Isatin	L	Spheres—long thin needles
<i>Enzymes</i>			
37	Acid phosphatase	L	Long thin needles
60	Aldolase	L	Dense spheres—elongate thin needles
38	α-Amylase	M	Long broad needles
39	β-Amylase	L	Long broad needles
40	Amyloglucosidase	L	Long very broad needles
41	Catalase	M	Spheres—short thin needles

Table 1 (continued)

Experiment No.	Chemical	Quantity of precipitate	Features
61, 140	Cellulase	L	Spheres—large thick needles; spheres—small thin needles
62	Deoxyribonuclease	L	Med. long very thin needles
42	Diastase/clarase	L	Small, long thin needles
43	Enterokinase	L	Dense spheres—thin short needles
44	Erepsin	L	Very long thin needles
45	Glucose oxidase	L	Med. long very thin needles
46	Invertase (bakers' yeast)	M	Tiny spheres (0.012 mm dia.)—short thin needles
47	Lipase (hog pancrease)	L	Spheres—thin small needles
48	Macerase (<i>Rhizopus</i> sp.)	M	Large spheres—long broad needles
49	Maltase (<i>Aspergillus niger</i>)	S	Calcite with long induction time, no gel
50	Papain (Papaya)	L	Med. long very thin needles
51	Pectinase (fungal)	L	Med. long very thin needles
52	Pepsin	L	Med. long very thin needles
53	Pronase	L	Spheres—long thin and med. wide needles
54	Protease	ML	Small, very thin needles
55	Pyruvate kinase (rabbit)	M	Med. long, med. thick needles
56	Rennet	L	Large spheres—needles
58	Trypsin	L	Spheres—med. long needles
59	Urease	L	Spheres—med. long very thin needles

Table 1 (continued)

Experiment No.	Chemical	Quantity of precipitate	Features
Sugars and sugar-based compounds			
15, 275	L-Arabinose	Tr	Clusters—short med. thick prisms
135	Cellobiose	L	Spheres—long thin needles, insoluble
23, 193	D-Fructose	S	Large dense spheres—Et; dense spheres—short, thick calcite
132	D(+)-Glucose/dextrose	L	Clusters—long, med. thick needles
21	D-Lactose	S	Large needles and tiny needles
22	D-Maltose	M	Large needles
27	D-Mannitol	M	Long (>0.24 mm) thin needles
157, 282	D-Rhamnose	S	Spheres—long med. thick needles
156, 283, 291	D-Ribose	S	Short thick hexagonal prisms
113	D-Sorbitol	S	Short med. thick needles
16	D-Sucrose	M	Small thin needles
32	Xylan	M	Bundles of med. needles
24	D-Xylose	S	Clumps—short broad prisms
20	Inulin	L	Large needle
110	Inositol	M	Spheres—thin and thick needles
111	myo-Inositol	L	Very thin needles
185	Starch (potato)	L	Very long med. thick needles with rounded tips
81	Arabinic acid	M	Clusters—short med. thick crystals with rounded tips
168	Gum arabic	S	Small spheres—short rounded needles

(continued on next page)

Table 1 (continued)

Experiment No.	Chemical	Quantity of precipitate	Features
108, 279	Galacturonic acid	S	Very short thick prisms
Phosphates and nucleotides			
90	Adenosine-2-monophosphoric Acid	M	Gel; calcite spheres, perhaps some AFm
133	ATP	L	Long very thin needles
181	Ammonium phosphate dibasic	—	Gel, no crystals after 8 months
170	Calcium phosphate tribasic	ML	Spheres—med. long, med. thick needles
97	Coccarboxylase (thiamine phosphate)-Cl	M	Gel; calcite spheres; long induction time
200	D-Glucose-6-phosphate	L	Gel; calcite; long induction time
206	Phosphocreatine	M	Large spheres—long thin crystals
205	Phosphoenol pyruvate	L	Large spheres—med. long med. thick crystals
175	M-Phosphoric acid	L	Spheres—needles
29	Potassium phosphate monobasic	—	Gel—stable for 9 months
29	Glycerol phosphate, Na	L	Large spheres—thin and thick needles
30	Hexametaphosphate, Na	—	Gel, no crystals after 9 months
8	Pyrophosphate, Na	L	Long (0.2 mm) needles
Vitamins			
122, 126	B ₁ Thiamine HCl	M	Spheres—med. long med. thin needles
125, 202	B ₃ Niacin (nicotinic acid)	L	Spheres—med. long med. thin needles
127	B ₆ Pyridoxine HCl	S	Spheres—med. long thin and thick needles
128	B ₅ Pantothenic acid	L	Long thin needles
71	B ₂ Riboflavin	L	Yellow dense clumps—radiating very thin needles

Table 1 (continued)

Experiment No.	Chemical	Quantity of precipitate	Features
96	Biotin	M	Spheres—long thin needles
Stains and related substances			
52	Acid Fuchsin	L	Spheres—long extremely thin needles
153, 227, 228, 240, 241, 242	Alizarin Red S	L	Long thin needles; AFm plates; short prisms
154, 220	Aniline blue	L	Ultra thin fiber-like needles
230	Azocarmine B	L	thin med. long (0.1 mm) needles
231	Basic Fuchsin (no SO ₃ Na)	L	med. thick long (0.21 mm) blue needles
232	Calmagite	L	Thin long (0.2 mm) needles
233	Congo Red	L	Thin fiber-like needles (0.12 mm long)
234	Cotton Blue	L	Thin fiber-like needles
235	Guinea Green	L	Med. thin, med. long needles
236	Evans Blue	L	Med. wide, long needles
237	Fast Green	L	Thin long (0.36 mm) needles
238	Indigo Carmine	L	Thin blue needles
239	Nuclear Fast Red	L	Spheres—long thin needles
77	2(2-Thiazolazo)- <i>p</i> -Cresol	L	Spheres—med. long very thin needles
130	1,4-Napthoquinone	ML	Long very thin needles
131	1,2-Napthoquinone	L	Clusters—med. long thin needles
Lignins and surfactants			
179	Dowfax 8390 (sulfonate)	L	Spheres—med. long thin needles

Table 1 (continued)

Experiment No.	Chemical	Quantity of precipitate	Features
180	Sandopan JA36	L	Spheres—long, thick and med. thick needles with pointed tips
220, 258	Polyfon O (lignosulfonate)	L	Small (0.009 mm dia.) spheres—AFm and short (0.001 mm) needles
221	Reax 6BW (lignocarboxylate)	S	Spheres—long (0.3 mm) needles
223	Reax 100 (lignosulfonate)	Tr	Large long needles
176, 284	Sodium lauryl sulfate	L	Immed. prec., voluminous gel-like flocks, ultrathin long fibers
301	WRDA-82 (lignosulfonate + amine water reducer/retarder), 2.2 ppt	M	Very short thick crystals; rounded tips + gel
302	WRDA with Hycol (lignosulfonate + amine formate/acetate, 2.2 ppt	M	Clusters—med. short med. thick
299	WRDA-82, 11 ppt	—	Gel
300	WRDA with Hycol, 11 ppt	—	Gel
Other substances			
13	Allantoin	M	Large and small long needles
99	AMO 1618	L	clusters—long thin needles
14	Amygdalin	ML	Spheres—long thin needles
124	BHT	L	Spheres—long thin needles
196	DL-Buthionine sulfoximine	L	Spheres—long thin needles with pointed (?) tips
169, 252	Casein	S	Spheres—small (0.024 mm long) med. thin needles
10, 116	Choline	L	Long thin needles

Table 1 (continued)

Experiment No.	Chemical	Quantity of precipitate	Features
172	Coumarin	M	Spheres—long med. thick needles
117	Cytidine	M	Clusters—short thick needles
100	DNA, Na	M	Clusters—med. long thin needles
107	Dicumarol	L	Spheres—med. long broad needles
173	Esculin	L	Spheres—thin needles
174	Ethylenediammonium sulfate, Fe ⁺²	ML	Spheres—med. long med. thick needles; gel
136	Ficin	L	Spheres—short (0.07 mm) very thin needles; gel
102	D-Glucose amine HCl	M	Clusters—med. long thick needles
109, 271	D-Glucuranoalactone	M	Spheres—long thick needles
224	Haematoxylin	L	Long needles
138	Kanamycin	ML	Spheres—med. long (0.09 mm), med. thick and thin needles
25	Proteose peptone	M	Spheres—exceptionally long thick needles
129	Sequestrene	L	Med. long very thin needles
57	Streptomycin	L	Dense spheres—large thick needles; trace gypsum
189	THAM	L	Med. long, med. thin needles
73, 190	Thioacetamide	L	Large spheres—med. long wide needles
208	Thiourea	L	Spheres—med. long med. thick needles
123	Thymidine	L	Spheres—long thin needles

Abbreviations: Quantity: L=large; M=medium; S=small; Tr=trace. Features: med.=medium; amt.=amount; dash (—)=composed of ...; dia.=diameter.

Ettringite crystals grown in solutions without additives are long, medium wide, six-sided in cross section (Fig. 2A), have flat terminations, and appear in large quantities (L). Single-valent ions, such as Li and K, have little effect on ettringite. NH_4 , Ba, Co, Cr, Mn, Pb, ZrO, and Ni cause long very thin crystals to form (Table 1). Although some of these ions are capable of substituting in the ettringite structure, their influence is believed to be mostly a surface effect. This will become clearer after the effects of other additives are examined.

Chen and Mehta [19] conducted zeta potential measurements of the surface charge on ettringite crystals and found it be negative (-11.6 mV) at pH 7, and even more negative (-13.4 mV) at pH 10.4 in 10^{-3} M $\text{Ca}(\text{OH})_2$. They concluded that this was due to adsorbed layers of water and/or hydroxide ions on the long crystal surfaces. It would not be unreasonable to imagine highly charged positive ions being attracted to the long crystal surfaces where they would shield the faces from further growth layers. Growth layers added to the ends of the needlelike crystals would result in the very elongate thin morphology that was observed.

Magnesium ions are closest in size to Ca ions and would most easily substitute for them in the crystal structure. Lerch et al. [20] found that ettringite crystals were unstable in solutions of magnesium salts where they dissolved. They do not indicate whether they adjusted the pH of the acidic magnesium solutions so that they were in the pH range where ettringite is stable. In our experiments with adjusted pH, crystals grown with Mg chloride were short (0.03 mm long) and thin.

Crystals formed in several experiments are pointed or show rounded terminations (Fig. 2B) and have formed by the chlorides of ions capable of substitution in the crystal structure, by the chloride ion itself (HCl), and by certain carboxylic acids (Table 1). Possibly, the negatively charged ions were attracted to the crystal edges where the short sides of the long rectangular $\{10\bar{1}0\}$ faces meet the six-sided end faces.

3.2. Carboxylic acids and borates

Carboxylic acids were tested because they were found to be very effective in altering the growth of many calcium minerals including gypsum [21] and the calcium oxalates [22]. Carboxylic acids can bind to calcium ions on the crystal surfaces to prevent further growth on those surfaces. Molecules with carboxylate spacing equal to the calcium spacing of the mineral were the most effective in preventing this growth. Citrate and tartrate ions are also powerful chelators of solution Ca^{2+} and Al^{3+} and would be expected to influence the nucleation and growth of phases containing these ions. Tartaric acid and its salts are used as Type B (ASTM C494) set retarders. Hydroxylated carboxylic acids, discussed here in the sugar section, are used as Type A (ASTM C494) water reducers [2] and citric, tartaric, gly-

colic, salicylic, heptonic, and malic acids have all been used as water-reducing plasticizers [1].

Most carboxylic acids had no effect on the morphology of ettringite crystals. This probably results from the fact that the calcium ions of the crystals are buried in a sheath of negatively charged hydroxyl and water molecules (Fig. 1) and the negatively charged carboxylate groups appeared to be repelled by the negatively charged crystals. The chelator molecules citrate and tartrate, as expected, affected the nucleation of ettringite. Fewer crystals were formed and the crystals were short because the nutrients for their growth were chelated. There is also the possibility that molecules chelated to calcium ions, which become part of the crystals, blocked rapid growth on the terminal faces. Short ettringite needles and a small quantity of the AFm phase were formed when a small quantity of isocitric acid was tested.

Salicylic acid is used as a set retarder because of its ability to complex aluminum [23]. Fewer ettringite crystals nucleated and they grew to a large size, but their morphology was not altered. Some AFm crystals were also observed suggesting that salicylic acid is an inhibitor of ettringite nucleation.

A concentration of 0.22 ppt mucic/galactaric acid produced pointed ettringite crystals. A greater mucic acid concentration of 0.66 ppt formed a long-lasting gel, indicating this to be a powerful nucleation inhibitor of both ettringite and the AFm phase.

Borax is used as a Type B (ASTM C494) set retarder. Borate ions are known to partially substitute for sulfate ions in the lattice of ettringite to form the minerals sturmanite and charlesite. Both boric acid and its sodium salt inhibited the nucleation of ettringite, but allowed six-sided plates of the metastable AFm phase to form instead. This is significant because if metastable primary AFm is formed in concretes in which borax is used as a set retarder, there is the possibility that it could easily convert over time to deleterious secondary ettringite. It would be of interest to know if the reported cases of concretes with primary monosulfate (or monosulfate that allegedly converted from ettringite) were concretes that were made with borax or the lignosulfonate inhibitors to be discussed later. A concentration of <44 ppm borax was capable of inhibiting ettringite and producing only the AFm phase. At no time was the barrel-shaped ettringite morphology, shown in Fig. 9 of Coveney and Humphreys [24], ever observed.

3.3. Amino acids and NH compounds

Amino acids and NH compounds were tested because they form both negatively charged carboxylate groups and positively charged NH_2^+ and NH_3^+ groups on relatively large organic molecules. The positively charged groups may adsorb onto negatively charged crystal faces and allow the large molecules to shield and prevent growth on those faces. Nearly all of the compounds tested produced long thin

ettringite crystals, indicating they were attracted to the negatively charged elongate crystal faces.

3.4. Enzymes

Enzymes are formed in concrete in small quantities produced mainly via microbiological processes. The effect of these very large molecules on the formation of ettringite in concrete has not been tested previously.

Many enzymes produced very thin needles, as might be expected, because they are composed of amino acids, which were found to produce very thin needles of ettringite. Maltase, enterokinase, lipase, and protease were unusual in producing large quantities of spherical crystal aggregates composed of relatively short ettringite needles. These chemicals are interpreted to be nucleation enhancers. When a large quantity of crystals nucleates, each individual crystal will have less nutrient to grow to large size. Rapid nucleation can be caused by a nucleation enhancer or by high supersaturation. Mehta [25] observed that ettringite forms slender needles and spherulites in solution growth and in high w/c experiments, but short prisms formed in low w/c experiments where the supersaturation is much higher and rapid nucleation of a greater number of crystals is expected.

3.5. Sugars and sugar-based chemicals

Sugars have been studied extensively because of their effects in retarding set time, especially in hot weather and in deep geothermally heated oil wells. Taylor [1] suggested that “sugars are capable of attacking concrete by complexing with calcium with consequential dissolution of CH and hydrated silicate and aluminate phases.” Thomas and Birchall [26] described three categories of retarding sugars: (1) trihalose and α methyl glucosides that are ineffective; (2) glucose, maltose, lactose, and cellobiose, which are good retarders, and (3) sucrose and raffinose, which are outstanding retarders. Thomas and Birchall [26] believed that sugars shield the surfaces of CH and thereby delay its dissolution and the rate of the setting reactions.

Sugars are capable of complexing calcium and possibly aluminum because they contain numerous hydroxyl groups that deprotonate to form multidentate negatively charged molecules, which in turn tightly bind positively charged solution ions. Ettringite formation is additionally prevented because the deprotonated hydrogen ions can lower solution pH below the pH stability range of ettringite. For this reason, control of solution pH was especially important in studying this group of additives.

In our experiments, the six-carbon (hexose) sugars that Thomas and Birchall [26] found to be effective in retarding total concrete set had little effect on ettringite growth. Struble [27] and Baussand et al. [13] did find high concentrations of sucrose (5%) to cause shortened crystals. Five-carbon (pentose) sugars such as arabinose, ribose, and

xylose were, however, found to be very effective in inhibiting both nucleation and growth of ettringite. In experiments, only a small quantity of crystals was formed and the crystals were short, thick, hexagonal prisms rather than needles. Degree of shortening of the prisms was found to correspond with the amount of pentose sugar added. Other chemicals that contained pentose sugar moieties (groups) were also effective in inhibiting crystal length. They included arabinic acid, galacturonic acid, adenosine, and cytidine. Sorbitol, a six-carbon, six-hydroxyl aliphatic sugar alcohol is used as a plasticizer because of its resistance to alkali attack. It was highly effective in inhibiting ettringite nucleation and linear growth.

Coveney et al. [28] proposed a model in which phosphonate compounds could delay cement setting by inhibiting the growth of ettringite by the mechanism of phosphonate groups substituting for and fitting into the lattice sites normally occupied by sulfate. Coveney and Humphries [24] designed and synthesized a ring-shaped “crown” triphosphonate molecule with the proper spacing of functional phosphonate groups to fit into the sulfate positions of the lattice on the terminal six-sided {0001} faces of the crystals. The ring shape of the crown triphosphonate molecule is analogous to the ring shape of pentose sugars that have hydroxyl functional groups in place of phosphonate groups. In the lattice structure of ettringite (Fig. 1A), there are three hydroxyl groups positioned between each calcium and aluminum ion. We first considered the possibility that sugar hydroxyl groups might fit into the lattice like the phosphonate groups proposed by Coveney et al. [28]. We later discarded this idea because the spacing of the three hydroxyl groups in the effective pentose inhibitors ribose, arabinose, and xylose was different in each case. There was also the consideration that if the hydroxyl groups of the sugar molecules were incorporated into the ettringite lattice, the remainder of the molecule would have to be overgrown by the crystal and would result in lattice and structural disruptions that would be visible. Because the crystals were perfectly transparent and showed no surface or optical disruption, it was concluded that the molecules were not overgrown but functioned by chelating calcium and possibly aluminum ions, which were incorporated into the crystals. The molecules’ shielding effect and their later detachment from the ions may have slowed the rate at which the crystals could grow to elongation. This conclusion is supported by the observations that sorbitol, tartaric and citric acids and their salts, all linear molecules that are known calcium chelators, were found in this study to inhibit ettringite nucleation and linear growth. Coveney et al. [28] state that the X-ray patterns of their shortened crystals “were entirely consistent with pure, well crystalline ettringite,” which would not have any obvious lattice disruption caused by overgrown phosphonate molecules. This raises the possibility that Coveney et al.’s expensive, tailor-made ettringite inhibitor may have only been a better calcium/aluminum chelator.

3.6. Phosphates and nucleotides

Certain phosphates have been added to concrete to reduce corrosion of steel reinforcement by chloride ions. Many of those tested here formed gels, showing that they were powerful Aft and AFm inhibitors. When potassium phosphate monobasic was added to aluminum sulfate and calcium hydroxide solutions in separate containers, a gel was formed in the hydroxide container indicating that a hydroxy, rather than an aluminate gel, was involved. Further detailed study of phosphates and nucleotides is warranted.

3.7. Sulfonated hydrocarbons and surfactants

Salts of lignosulfonates, alkylbenzene sulfonates, sulfonated hydrocarbons, and synthetic detergents are added to concrete as air-entraining admixtures and to improve workability (ASTM C260). Most of the biological stains tested in this study were sulfonated hydrocarbons of varied molecular weight and structure. Several also contained benzene rings. Stains containing between zero and four sulfonic acid groups were tested. Nearly all of the stains produced a large quantity of long thin needles indicating that they did not inhibit nucleation and that they were adsorbed along the long axis of the crystals. It is uncertain why molecules with negatively charged carboxyl groups had no effect on the growth of negatively charged ettringite crystals, whereas molecules with negatively charged sulfonic acid groups did. It is hypothesized that a sulfonic acid group may be incorporated into the crystal as a substitute for sulfate. The remainder of the molecule would then shield the sides of the crystal from rapid growth until the molecule is overgrown by layers of crystal growth. Linear surface and growth defects would be expected if this occurred. Crystals grown with Alizarin Red S (Fig. 2C) exhibit these defects on the edges between their long faces. Carboxylic acid groups are probably incapable of substituting for any of the lattice components in ettringite and so they have no effect on growth.

Commercial lignosulfonate chemicals had more powerful effects on ettringite than the biological stains. Polyfon O with one sulfonic acid group, inhibited ettringite, but allowed the metastable AFm phase to form. Again, as with borax, later decomposition of the metastable AFm phase could possibly contribute to the formation of secondary ettringite. Reax 6BW, a lignocarboxylate with 1.5 sulfonic acid groups produced very long (>0.3 mm) ettringite needles and behaved as a nucleation inhibitor, as did the lignosulfonate Reax 100.

The most extraordinary results were found when a very small quantity of the surfactant sodium lauryl sulfate (a sulfate ester) was tested. A large 3-cm block of dense latex-appearing “clot” formed in the solution and could be removed in one piece. It was found to consist of long, extremely fine fiberlike (asbestiform) crystals that could bend without breaking. When the mass dried, it shrank to

the size of a standard large quantity (L) precipitate, thus showing that much of the large initial volume was due to water adsorption. The fact that great water adsorption and expansion was seen with fiberlike crystals having large surface areas associated with the elongate crystal faces indicates that these faces play a major role in the expansion of ettringite during water adsorption. It is not just the larger surface area associated with small crystal size that causes large water-induced expansion [4], but rather it is the greater surface area of the elongate water-adsorbing $\{10\bar{1}0\}$ crystal faces that causes adsorption of large volumes of water. This observation may find application in the commercial use of ettringite to produce fire-resistant wallboard. Sodium lauryl sulfate is used as an air-entrainment admixture [3]. It also is a component of most detergents and it may be introduced into concrete if impure water is used.

4. Summary

A new method of crystal growth was devised to reliably produce ettringite crystals that could be seen with a light microscope ($45\times$ – $320\times$). Nearly 300 chemicals, many of which are present in the concrete environment, were tested to determine their effects on ettringite nucleation, growth, and morphology. Most carboxylic acids had no effect on ettringite except for the known calcium chelators (and water-reducing plasticizers) citrate and tartrate, which prevented both nucleation and growth. Hydroxylated carboxylic acids such as mucic/galactaric and its further-hydroxylated form, the plasticizer sorbitol, were very effective in inhibiting ettringite nucleation and growth. A smaller quantity of short, stubby ettringite crystals resulted. Pentose sugars also inhibited elongation growth, whereas hexose sugars, which are used as concrete set retarders, had little effect on ettringite nucleation and growth.

Sodium tetraborate (borax), which is used as a Type B set retarder, was found to inhibit ettringite nucleation at a concentration <44 ppm. Borax caused the metastable AFm phase to form instead. Commercial lignosulfonates chemicals were found to do the same. Further study is needed to determine if these reactions occur in concrete and if later conversion of the metastable AFm phase to ettringite contributes to the formation of secondary ettringite that many researchers conclude is responsible for serious premature deterioration of concrete highways.

Acknowledgements

This work was funded as Project TR-431 from the Iowa Department of Transportation whose support is gratefully acknowledged. We thank Mark Dunn, Wallace Rippie, and Robert Dawson of the Iowa DOT and Jim Myers and Wendell Dubberke for their advice, suggestions, and support. Max Porter of the ISU Civil and Construction Engineering

Department is thanked for his advice, and Jerry Amenson and Scott Schlorholtz of the ISU Materials Laboratory for their assistance with SEM analyses.

References

- [1] H.F.W. Taylor, *Cement Chemistry*, Academic Press, New York, 1990.
- [2] S.H. Kosmaka, W.C. Panarese, *Design and Control of Concrete Mixtures*, Portland Cement Association, Skokie, IL, 1988.
- [3] P.C. Hewlett (Ed.), *Lea's Chemistry of Cement and Concrete*, 4th ed., Wiley, New York, 1998.
- [4] P.K. Mehta, Mechanisms of expansion associated with ettringite formation, *Cem. Concr. Res.* 3 (1) (1973) 1–6.
- [5] P.J. Tumidajski, I. Turc, A rapid test for sulfate ingress into concrete, *Cem. Concr. Res.* 25 (5) (1995) 924–928.
- [6] S. Wolter, *Ettringite. Cancer of Concrete*, Burgess Publishing, New York, 1996.
- [7] R.D. Cody, A.M. Cody, P.G. Spry, H. Lee, Expansive mineral growth and concrete deterioration, Iowa Department of Transport, Final Report HR-384, 1997.
- [8] S. Diamond, Delayed ettringite formation—processes and problems, *Cem. Concr. Compos.* 18 (3) (1996) 205–215.
- [9] H. Lee, Expansive mineral growth and concrete deterioration: a microstructural and microanalytical study, PhD dissertation, Iowa State University, Ames, IA, 1999, 292 pp.
- [10] A.M. Neville, Behavior of concrete in saturated and weak solutions of magnesium sulphate or calcium chloride, *J. Mater.* 4 (4) (1969) 781–816.
- [11] P.K. Mehta, Mechanism of sulfate attack on Portland cement concrete—another look, *Cem. Concr. Res.* 13 (3) (1983) 401–406.
- [12] I. Odler, A. Maula, Possibilities of quantitative determination of the AFt(ettringite) and AFm(monosulphate) phases in hydrated cement pastes, *Cem. Concr. Res.* 14 (1) (1984) 133–141.
- [13] J.B. Baussant, C. Vernet, C. Defosse, Growth of ettringite in diffusion controlled conditions influence of additives on the crystal morphology, Proceedings 11th International Conference Cement Microscopy, April 1989, New Orleans, Internatl. Concrete Microscopy Assoc., Duncanville, TX, 1989, pp. 186–197.
- [14] E.T. Carlson, H.A. Berman, Some observations on the calcium aluminate carbonate hydrates, *J. Res. Natl. Bur. Stand., A Phys. Chem.* 64 (4) (1960) 333–341.
- [15] C.R.W. Mylius, Calcium aluminate hydrates and their double salts, *Acta Acad. Aboensis Math Phys.* 7 (3) (1933) 147.
- [16] D. Damidot, F.P. Glasser, Thermodynamic investigation of the $\text{CaO}-\text{Al}_2\text{O}_3-\text{CaSO}_4-\text{H}_2\text{O}$ system at 25 °C and the influence of Na_2O , *Cem. Concr. Res.* 23 (1) (1993) 221–238.
- [17] H.F.W. Taylor, Crystal structures of some double hydroxide minerals, *Min. Mag.* 39 (304) (1973) 377–389.
- [18] K. Ogawa, D.M. Roy, $\text{C}_4\text{A}_3\text{S}$ hydration, ettringite formation, and its expansion mechanism: effect of CaO , NaOH , and NaCl ; conclusions, *Cem. Concr. Res.* 12 (2) (1982) 247–255.
- [19] S.-S. Chen, P.K. Mehta, Zeta potential and surface area measurements on ettringite, *Cem. Concr. Res.* 12 (2) (1982) 257–259.
- [20] W. Lerch, F.W. Ashton, R.H. Bogue, The sulphoaluminates of calcium, *J. Res. Natl. Bur. Stand.* 2 (4) (1928) 715–731.
- [21] A.M. Cody, R.D. Cody, Chiral habit modifications of gypsum from epitaxial-like adsorption of stereospecific growth inhibitors, *J. Cryst. Growth* 113 (1991) 508–519.
- [22] S. Diamond, Interactions between cement minerals and hydroxycarboxylic-acid retarders: I. Apparent adsorption of salicylic acid on cement and hydrated cement compounds, *Am. Ceram. Soc.*, (1971) 273–277.
- [23] A.M. Cody, R.D. Cody, Calcium oxalate trihydrate phase control by structurally-specific carboxylic acids, *J. Cryst. Growth* 135 (1994) 235–245.
- [24] P.V. Coveney, W. Humphries, Molecular modeling of the mechanism of action of phosphonate retarders on hydrating cements, *J. Chem. Soc., Faraday Trans.* 92 (5) (1996) 831–841.
- [25] P.K. Mehta, Scanning electron micrographic studies of ettringite formation, *Cem. Concr. Res.* 6 (2) (1976) 169–182.
- [26] N.L. Thomas, J.D. Birchall, The retarding action of sugars on cement hydration, *Cem. Concr. Res.* 13 (6) (1983) 830.
- [27] L.J. Struble, Synthesis and characterization of ettringite and related phases, Congr. Int. Quim. Cimento, 8th, Secr. Gen. 8o CIQC, Rio de Janeiro, Brazil, vol. 6, Abila Grafica e Editova, Rio de Janeiro, 1986, pp. 582–589.
- [28] P.V. Coveney, R.J. Davey, J.L.W. Griffin, A. Whiting, Molecular design and testing of organophosphonates for inhibition of crystallization of ettringite and cement hydration, *Chem. Commun.* 14 (1998) 1467–1468.
- [29] R.L. Day, The effect of secondary ettringite formation on durability of concrete: a literature analysis, PCA Research and Development Bulletin RD108T, 1992, pp. 1–115.